Journal of Applied Fluid Mechanics, Vol. 15, No. 3, pp. 697-708, 2022.
Available online at www.jafmonline.net, ISSN 1735-3572, EISSN 1735-3645.
https://doi.org/10.47176/jafm.15.03.33357

Influence of Axial Position of Self-Circulating Casing Treatment on the Performances of a Centrifugal Pump at Low Mass Flow Conditions

H. Liu[1†], Y. Li[2], H. Chen[1, 3], Y. Wei[1], S. Lu[4], M. Jiang[1, 5] and G. Wang[5]

[1] *Marin Engineering College, Dalian Maritime University, Dalian 116026, China*
[2] *Key Laboratory of Biomechanics and Mechanobiology (Beihang University), Ministry of Education, Beijing Advanced Innovation Center for Biomedical Engineering, School of Biological Science and Medical Engineering, Beihang University, Beijing, 100083, China.*
[3] *Naval Architecture & Ocean Engineering College, Dalian Maritime University, Dalian 116026, China*
[4] *Jiangsu Haiming Medical Equipment Co., Ltd, Yangzhou, 225101, China*
[5] *Danai Pumps Co. Ltd, Dalian 116630, China*

†*Corresponding Author Email: huachen204887@163.com*

(Received September 10, 2021; accepted January 3, 2022)

ABSTRACT

Centrifugal pumps often deviate from its design condition during its operation and work at low mass flow conditions. Under such circumstances, unstable flow phenomena may be generated, affecting the efficient and stable operation of pumps. In this paper, a self-circulating casing treatment in U-tube shape is employed on a centrifugal pump to study its effects on the pump's performance by computational and experimental studies. CFD results show that as the flow rate decreases, the back-flow in the inlet pipe of the studied pump without casing treatment increases in intensity and spreads over an growing distance, interfering with the main flow. CFD results also reveal that the casing treatment has a sucking function to the back-flow due to the blade loading of the pump, and when the inlet bleed of the U-tube is placed above (in front of) the leading edge of the blades, the sucking is the strongest, and the control of the back-flow and the improvement to the head coefficient under low mass flow conditions is the best, as the vortex blockage caused by the sucked back-flow in the U-tube is the smallest; when the bleed is under (after) the leading edge of the blades, the effect of the casing treatment is the second best; and when the bleed is across the leading edge of the blades, the blockage in the U-tube is most severe, and the sucking function is the weakest, so there is little improvement to the back-flow and head coefficient. Finally, the reliability of this study was demonstrated employing an open pump experimental system with the original pump and the same pump with the casing treatment whose bleed is located above the leading edge of the impeller.

Keywords: Centrifugal pump; Self-circulating casing treatment; Back-flow; Axial position.

NOMENCLATURE

$D2$	impeller outlet diameter
H	head
Q	mass flow rate
Z	number of blades
$\beta 2$	blade outlet angle
Ψ	wrap angle
η	efficiency
Ω	rotation speed

Subscripts

d	design condition
ori	original (pump)
s	sucking function
CFD	Computational Fluid Dynamics
LE	leading edge
$U\text{-}tube$	U-tube treated (pump)

1. INTRODUCTION

The operation of centrifugal pumps is influenced by various factors, and pumps may deviate from their design mass flow condition and operate at low mass flow conditions. There are a number of unstable flow phenomena within a centrifugal pump operating at low flow conditions that have a negative impact on the operation of the pump. For example: (1) the energy consumption and the cavitation caused by

back-flow, which leads to the degradation of the performance of centrifugal pump; (2) the low frequency pressure pulsation induced by the unstable flow, which generates noise and mechanical vibration; (3) in some low mass flow conditions stall and surge will occur, which destroys the uniformity of the internal flow field and seriously affects the safe operation of the pump. Therefore, to improve the internal flow state of centrifugal pumps at low mass flow conditions is of great significance to the hydraulic performance and safety of centrifugal pump operation.

As to the mechanism of back-flow in centrifugal pumps, Stepanoff (1998) suggested that the presence of inertial forces caused an increase in the circumferential velocity of the fluid near the impeller inlet, which disrupted the energy gradient required for fluid flow along the streamline, leading to the occurrence of inlet back-flow. Fraser *et al.* (1981) believed that back-flow occurs because as the flow rate decreases, a reverse pressure gradient occurs at certain points on the Q-H curve, causing the fluid to flow backwards. Schiavelo *et al.* (1983) attributed the generation of back-flow to a deliquescence near the inlet side of the front cover of the impeller. The presence of back-flow not only affected the hydraulic characteristics of the pump, but also the safe and stable operation of the pump. Li *et al.* (2014) found that as the flow rate decreased, the impeller inlet back-flow gradually expanded and stalls were observed in the impeller passages. Si *et al.* (2013) found that back-flow induced low-frequency pressure pulsation, which was the main cause of pump operating noise. Tsujimoto *et al.* (1997, 2013, 2002, 2007) observed back-flow-induced cavitation and the generation of low-frequency pressure pulsations in their experiments.

In terms of back-flow control, Cooper *et al.* (1984) proposed installing a back-flow slotting in the inlet pipe to control back-flow. Oshima (1967) and Toyokura and Kubota (1969) installed an orifice plate in front of the inlet of a pump with an inducer to weaken back-flow. Zhang *et al.* (2012) introduced high pressure water at the inlet pipe to reduce the intensity of back-flow, but this adversely affected the flow field of the pump. Cheng *et al.* (2016) broke the back-flow vortex by adding a front guide vane. Li *et al.* (2019) found that increasing the impeller surface roughness could homogenise the velocity and reduce the strength of the impeller inlet back-flow.

The casing treatment is a means of improving the operational stability of compressors, and is divided into two forms: circumferential casing treatment and self-circulating casing treatment. The circumferential casing treatment has been applied to centrifugal and axial pumps and has been found to control the blade leakage vortices in centrifugal pumps, thereby weaken rotating stalls Guo (2019). It has also been found that circumferential casing treatment is beneficial in improving the pump hump phenomenon and improving the stability of pump operation (Feng *et al.* 2018). Gonzalez *et al.* (2002) installed a J-slotting in the end-wall of the outlet pipe of a pump and found it to be effective in suppressing the pump surge. As for the self-circulating casing treatment, Current authors (Li *et al.* 2020, 2021) have applied a self-circulating casing treatment to a double-volute type centrifugal pump and found that it improves inlet back-flow and reduces low-frequency pressure pulsations caused by asymmetrical volute. Chen and Lei (2013) provide a detailed discussion of its application to centrifugal compressors and point out that its axial position has an important influence on the stable operation of centrifugal compressors. In this paper we continue to discuss the influence of the axial position of this type of casing treatments on the back-flow control and hydraulic performance of centrifugal pumps.

2. THE PUMP STUDIED

2.1 Original pump

The original pump is a centrifugal pump whose 3D solid model is shown in Fig. 1. The model mainly consists of: inlet pipe, closed or shrouded impeller, front-side cavity, back-side cavity, volute, wear-ring and balance pipes/holes. The design information of the pump is given in Table 1.

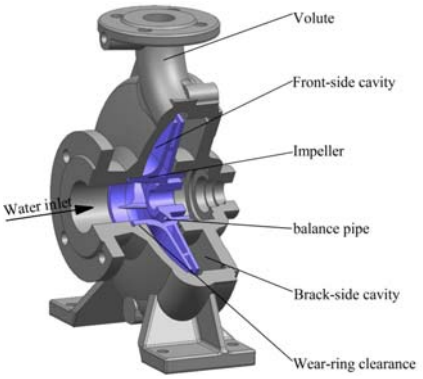

Fig. 1. 3D model of original pump.

Table 1. Main design parameters of studied pump

Description	Parameters	Value
Design flow rate (kg/s)	Q	9
Design head (m)	H	77
Design efficiency (%)	η	52%
Rotation speed (RPM)	Ω	2900
Number of blades	Z	5
Blade outlet angle (°)	β_2	35
Wrap angle (°)	Ψ	110
Impeller outlet diameter (m)	D_2	0.254

2.2 The pump with casing treatment

The pump with a self-circulating casing treatment is illustrated in Fig. 2. The front cover of the impeller and the inlet casing end-wall are both grooved, thereby forming a U-tube type flow passage. The U-tube connects the impeller near the leading edge with the inlet pipe, and may bypassing the leading edge of the impeller if the bleed is to the left of the leading edge. In order to hold the position of the ring structure of the U-tube, three circumferentially

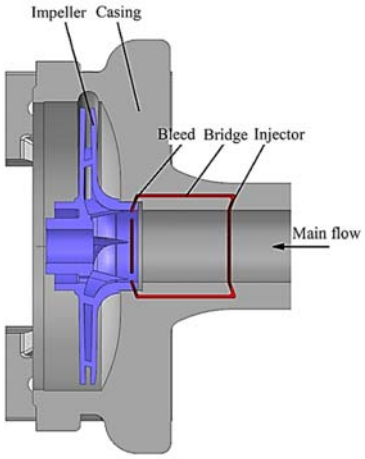

Fig. 2. U-tube type of self-circulating casing treatment on the studied pump.

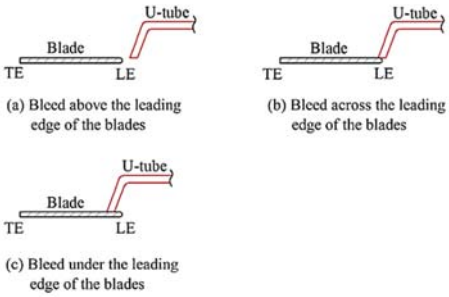

Fig. 3. Three different grooving positions on the front cover of the impeller relative to the leading edge of the blades.

distributed supporting ribs are employed to connect the U-tube and inlet pipe casing. The influence of the length of the casing treatment has been analyzed in our previous study (2020). In order to explore the best grooving position on the front cover of the impeller, three representative positions, bleed inlet above or to the right of the leading edge of the impeller blades, bleed inlet across or on the top of the leading edge of the blades and bleed inlet under or to the left of the leading edge of the blades, as shown in Fig. 3, were selected for comparison.

3. SIMULATION METHOD

3.1 Steady Numerical setting

The interior flow of the centrifugal pump is a turbulent flow of three-dimensional, incompressible viscous fluid. The governing equations used are the Reynolds Averaged Navier-Stokes (RANS) equations. The equations were solved using commercial software CFX® which employs a finite-volume method based discretization of the governing equations. The convection term was solved in the high resolution format, and the standard k-ε turbulence model and the Frozen-Rotor interface was adopted in the steady study. The boundary conditions of the inlet of Standard Ambient Pressure and Temperature of 101.325 kPa and 25ºC, and the mass flow outlet were imposed, and all the solid walls were assumed no slip, smooth and adiabatic. The convergence criterion was set to 10^{-8}.

3.2 Mesh details and independence verification

There are many computational domains of the centrifugal pump whose geometrical shape is complex, so this paper adopts tetrahedral unstructured meshes which have better adaptability to the boundary, and the y+ is less than 10 to meet the requirements of k-ε turbulence model.The meshes of impeller and the casing treatment are shown in Fig. 4. The need for boundary-layer type meshes for solid sur-faces are taken into consideration, and complex geo-metric regions are locally refined. Three mesh densities were analyzed for grid density independence: coarse (C), medium (M) and fine (F). The medium mesh totaled 12 million cells. The total number of cells was then reduced and increased by a factor of one to generate the coarse and the fine meshes. Since this paper focuses on low mass flow conditions, 0.22Qd where Qd is design flow rate is selected for mesh independence verification and the results are given in Table 2. It can be seen that the medium and fine mesh densities differ little on the head and efficiency. Thus, the medium mesh was chosen as a trade off between accuracy and wall-clock time.

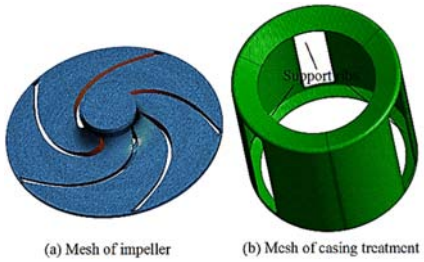

Fig. 4. Mesh of impeller & casing treatment (U-tube).

Table2. Grid independence verification

	Head Ratio (Relative to that of fine mesh)	Efficiency Ratio (Relative to that of fine mesh)
C-F	0.8686	0.9398
M-F	0.9928	1.0016

4. SIMULATION RESULTS ANALYSIS

4.1 Influence of axial position on the flow in the inlet pipe

In order to investigate the influence of different axial positions on the control of back-flow in the studied pump, the flow in the inlet pipe with and without casing treatment at four different mass flow rates, $0.11Q_d$, $0.22Q_d$, $0.44Q_d$ and $0.66Q_d$ is illustrated in Fig. 5-8.

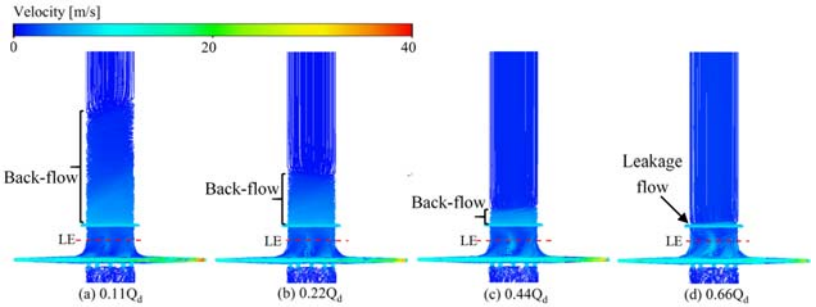

Fig. 5. Velocity and streamline distributions of inlet pipe when without casing treatment.

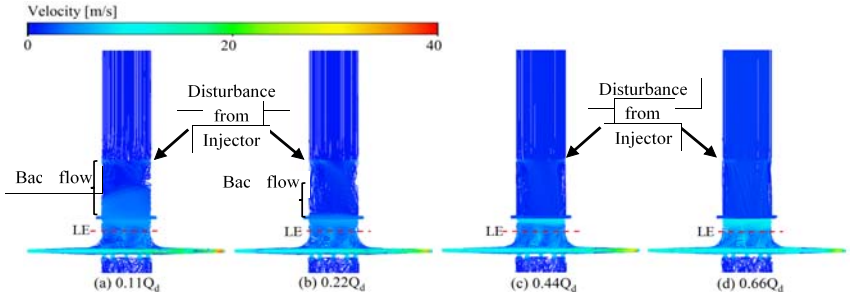

Fig. 6. Velocity and streamline distributions of inlet pipe when the bleed of casing treatment is above the leading edge of the impeller.

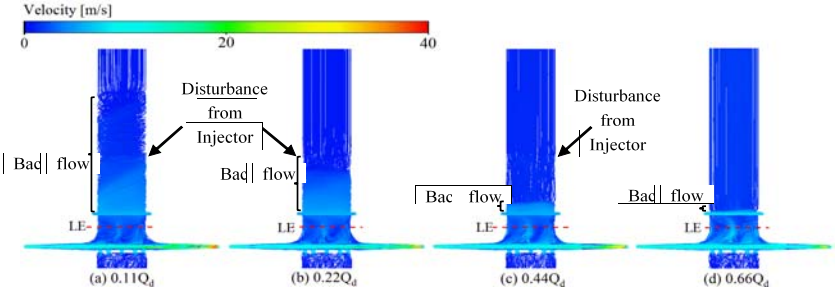

Fig. 7. Velocity and streamline distributions of inlet pipe when the bleed of casing treatment crosses the leading edge of the impeller.

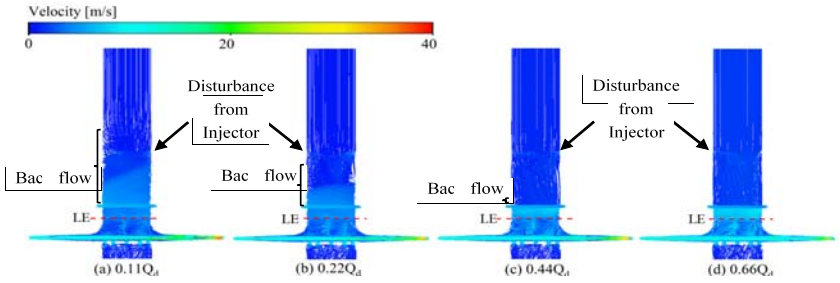

Fig. 8. Velocity and streamline distributions of inlet pipe when the bleed of casing treatment under the leading edge of the impeller.

As shown in the Fig. 5, when without casing treatment, there is almost no back-flow in the inlet pipe at the mass flow rate of 0.66Qd (back-flow is begin to be observed at this flow rate.). When the mass flow rate drops to 0.44Qd, a clear irregular back-flow appears on the end-wall of the inlet pipe, but at this flow condition, the back-flow spreads over only a short distance and has a relatively minor crowding effect on the mainstream. As the mass flow rate is further reduced to 0.22Qd, the back-flow is more conspicuous and spreads backwards to about twice the pipe diameter, and has a more crowding

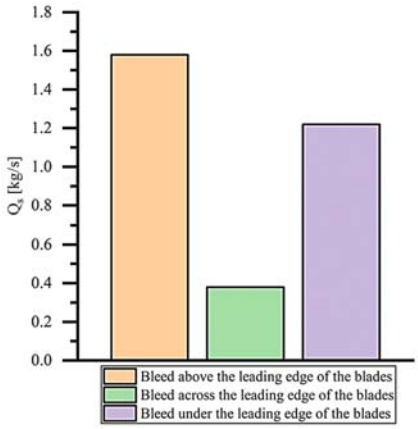

Fig. 9. Variation of self-circulating flow rate with axial position of the bleed.

effect on the mainstream. As the mass flow rate continues to drop to 0.11Qd, the back-flow extends to approximately three times the pipe diameter and the crowding effect on the main flow is further boosted. So, based on the above observation, the back-flow intensifies with decreasing mass flow, so too the distance of the reverse spread and its disturbances to the mainstream.

Figures 6-8 show the influence of three different axial positions of bleed on the control of back-flow at different mass flow conditions. As the flow rate decreases, the back-flow intensity also increases continuously, the control effect of the three axial positions of the casing treatment appears different: the best control of back-flow is when the bleed is above the leading edge of the blades: the back-flow travels less upstream and its velocity is greatly reduced; the second best is when the bleed is under the leading edge of the blades; and the worst one is when the bleed across the leading edge. At 0.11Qd mass flow condition, all the casing treatments fails to completely eliminate the back-flow in the inlet pipe. It is also found that although the casing treatment is reducing or eliminating back-flow, it also adds some new swirls to the inlet pipe through its injector.

4.2 Influence of axial position on the flow in the U-tube

Due to the stable presence of back-flow at 0.22 Q_d mass flow condition and the representative control of back-flow by the three casing treatments of Bleed at this flow, the flow condition at 0.22 Q_d was chosen for the following study to understand the control mechanism to the back-flow and the mechanism causing the different results from the three axial positions of the treatment.

To investigate the reasons for the influence of the axial position of the bleed on the back-flow, the suction of the casing treatment at 0.22Qd mass flow condition is looked into and the mass flow through the U-tube is shown in Fig. 9. It is found that the maximum self-circulating flow from the U-tube is generated when the bleed is above the leading edge of the blades, the second highest flow is when the bleed is under the leading edge of the blades, and the smallest flow is when the bleed across the leading edge of the blades. The amount of the recirculating flow is thus directly linked to the control of the back-flow in the front of the impeller.

To understand the reason for these differences in the recirculating mass flow, Fig. 10 shows the flow in the U-tube at the three different axial positions of the bleed. It can be seen that there are vortices inside the U-tube generated by large incidences of the flow from the bleed onto the three straight supporting ribs, as the flow has obtained some tangential momentum from the rotating impeller. These vortices form blockages to the recirculating flow. When the bleed is above the leading edge of the blades, the flow entering the bleed will have less swirl and hence smaller incidences on to the ribs, resulting weaker flow separations, smaller vortices and less blockages to the flow in the U-tube, as shown in Fig. 10(a); When the bleed is located across the leading edge of the blades, the flow entering the bleed in almost tangential direction, this creates large incidences and severe flow separations downstream, generating the largest vortices and strongest blockages in the U-tube, as shown in Fig.10(b); When the bleed is located under the leading edge of the blades, the flow entering the bleed will have the highest tangential momentum, but it will also have the largest axial momentum, for the pressure gradient across the U-tube will be the greatest due to blade loading; the combination of these two factors produces the largest flow velocity inside the U-tube, and although vortices blockages to the flow is severe, the U-tube can still be effective, as shown in Fig. 10(c). This analysis shows ways forward to reduce the incidence to the ribs and improve the recirculation: shorten the rids and place them away from the bleed to reduce the area of incidence, align the ribs with the incoming flow to reduce the incidence angle and at the same time choose appropriate camber for the ribs to gradually turn this flow to axial direction.

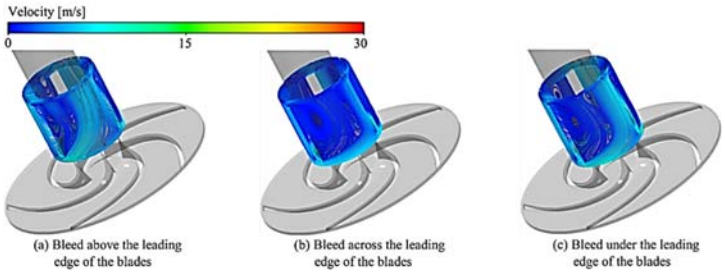

Fig. 10. Effect of axial position of the bleed on the flow in the U-tube.

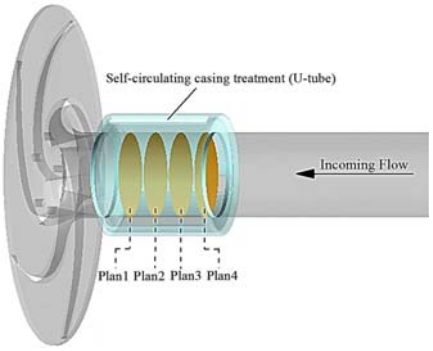

Fig. 11. Relative position of different selected plans in inlet pipe.

4.3 Influence of axial position on the total pressure in the inlet pipe

Four different plans were taken of the inlet pipe in between the impeller inlet and the injector of the U-tube, as shown in Fig. 11, to observe the total pressure distribution with and without casing treatment at 0.22Qd mass flow condition.

As shown in Fig. 12, when without casing treatment, Planes 1-3 are clearly influenced by the back-flow and their total pressure distribution is high near the end-wall and low at the center: the back-flow from impeller carries the work done by the impeller with it. And the closer to the impeller inlet, the more pronounced this characteristic becomes. Plane 4 is less affected by back-flow due to its distance from the impeller inlet, so the pressure distribution there is more even.

Figures 13-15 show the influence of different axial positions of the bleed on the total pressure distribution in the inlet pipe. The total pressure distribution in the inlet pipe is more uniform at Plans 1-2 with all the casing treatments as the sucking function of the U-tube reduces or eliminates the back-flow in the inlet pipe. The pressure distribution in all of Planes 1-4 is most uniform when the bleed is above the leading edge of the blades; and the second best case is when the bleed is placed under the leading edge; when the bleed is located across the leading edge, the total pressure in Planes 1-2 still shows a forced-vortex type nonuniform distribution. There are three distinct high-low total pressure areas, particularly in Plane 4 regardless axial positions of the bleed, this is thought to relate to the addition of new flow swirls by the casing treatment through the injector and the existence of the three supporting ribs.

4.4 Influence of axial position on the static pressure in the inlet pipe and impeller

The static pressure distribution below 100,000Pa (inlet pressure is 101,325Pa) in the impeller and inlet pipe at $0.22Q_d$ mass flow condition is illustrated in Fig. 16. When without the casing treatment, the shroud region of the pipe close to the impeller is blocked by the back-flow so the fluid enters the pump through unblocked hub region with increased velocity and reduced pressure, Fig. 16(a). The axial and radial spans of this low pressure zone decreases with the casing treatment. Different bleed inlet axial positions have different effects on the size of the low pressure zone: the best control of the back-flow is when the bleed is located above the leading edge of the blades, and therefore the low pressure zone is

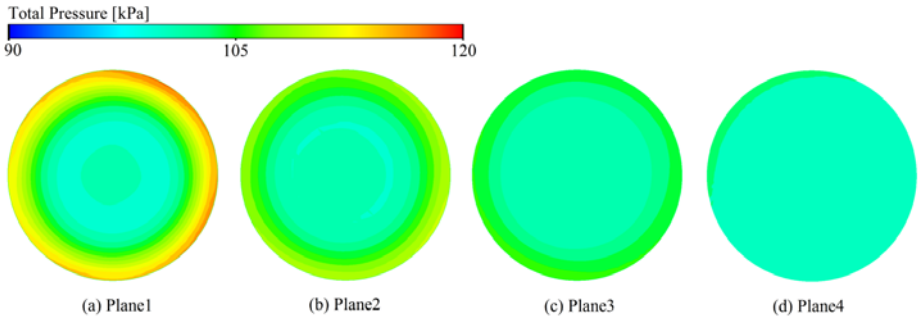

Fig. 12. Total pressure distribution in inlet pipe when without casing treatment.

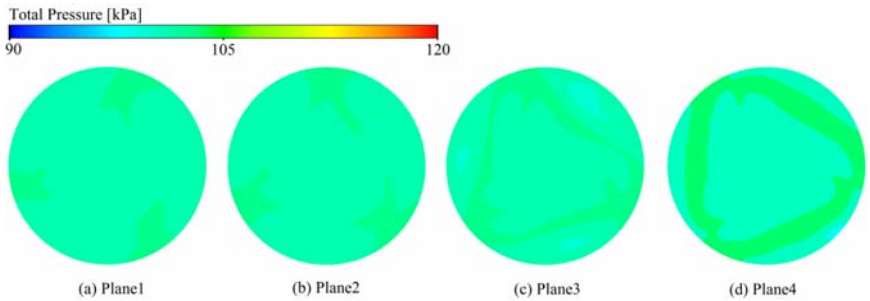

Fig. 13. Total pressure distribution in inlet pipe when the bleed of casing treatment is above the leading edge of the impeller.

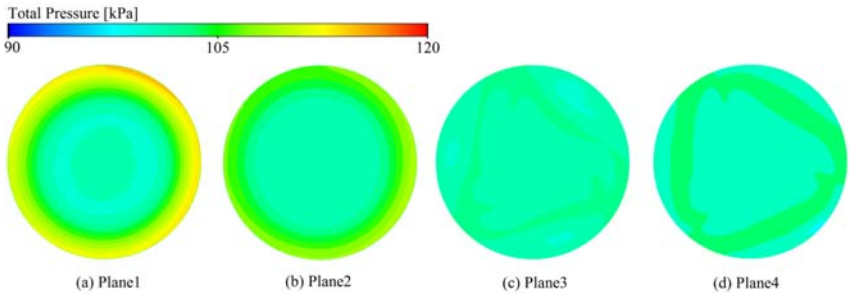

Fig. 14. Total pressure distribution in inlet pipe when the bleed of casing treatment crosses the leading edge of the impeller.

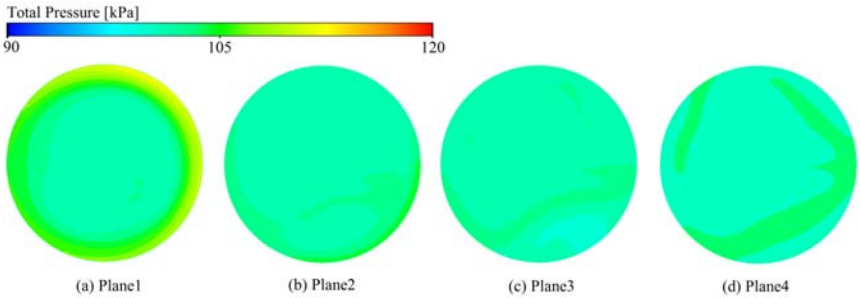

Fig. 15. Total pressure distribution in inlet pipe when the bleed of casing treatment is under the leading edge of the impeller.

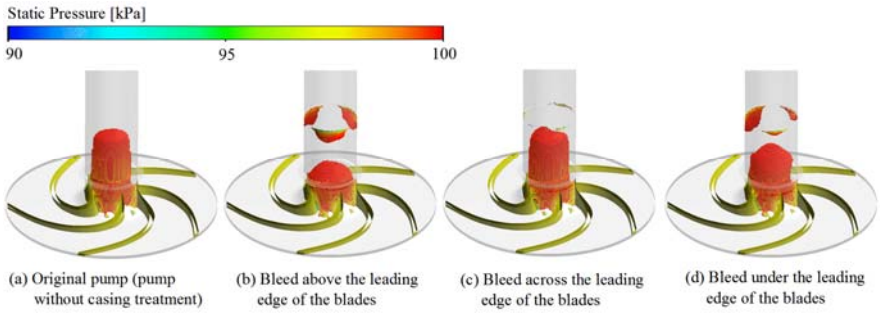

Fig. 16. Static pressure distribution in inlet pipe & impeller with and with casing treatment.

smallest in this case, Fig. 16(b), the injection of the recirculated flow creates three localized low pressure zones further upstream; When the bleed is across the leading edge of the blades, there is less fluid flowing from the U-tube as the blockage in the U-tube is at its worst, Fig. 16(c), so the low pressure zone at the center is almost as large as the case without the casing treatment, and the injector outlet is also nearly unaffected.

According to studies (Yuan *et al.* 2018; Yamamoto *et al.* 2009; Ito *et al.* 2015), cavitation in the inlet pipe of centrifugal pumps at low mass flow conditions is closely linked to back-flow. The casing treatment used here reduces or eliminates back-flow in the inlet pipe, resulting in the disappearance or reduction of the low pressure zone in the inlet pipe, this suggests the casing treatment may be beneficial in controlling cavitation at low mass flow conditions caused by back-flow.

4.5 Influence of axial position on the entropy production in the inlet pipe

Figures 17-20 show the distribution in entropy production in the inlet pipe with and without casing treatment at $0.22Q_d$ mass flow condition. The four plane locations are shown in Fig. 11. When without casing treatment, the losses are greatest on Plane 1, the plane closest to the impeller, as shown in Fig. 17(a), because of the high intensity of the back-flow near the impeller leading edge; and the losses occur in shroud region where the back-flow is the strongest. As the back-flow is impeded by viscous drag spreading through the inlet pipe, its forward momentum gradually decreases, (see Fig. 5(b)), and so does the resulting loss, as shown in Fig. 17(b)-(d). After employing the casing treatment, when the bleed is located above the leading edge of the blades, the losses in the Planes 1 and 2 are significantly reduced as shown in Fig. 18 and are the smallest among all the cases here; In Planes 3 and 4 that are

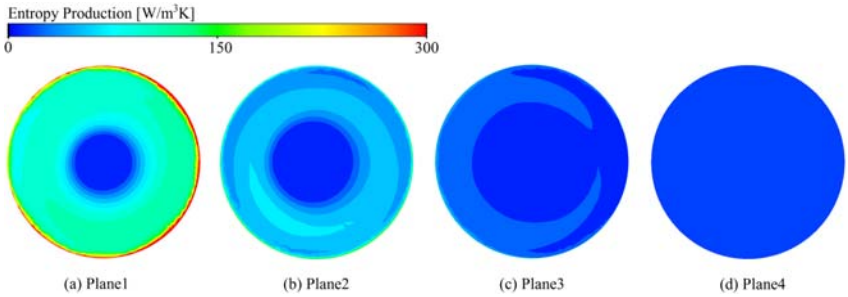

Fig. 17. Entropy production in inlet pipe when without casing treatment.

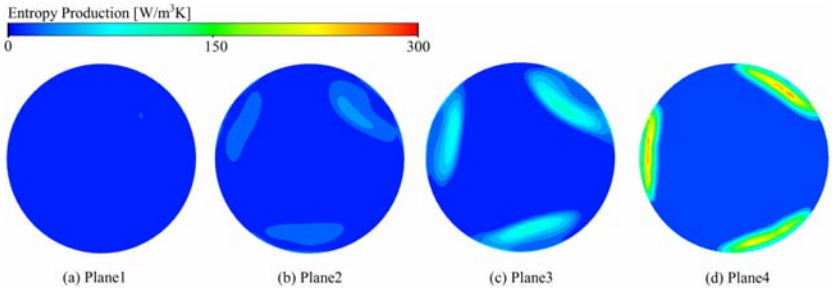

Fig. 18. Entropy production in inlet pipe when the bleed of casing treatment is above the leading edge of the blades.

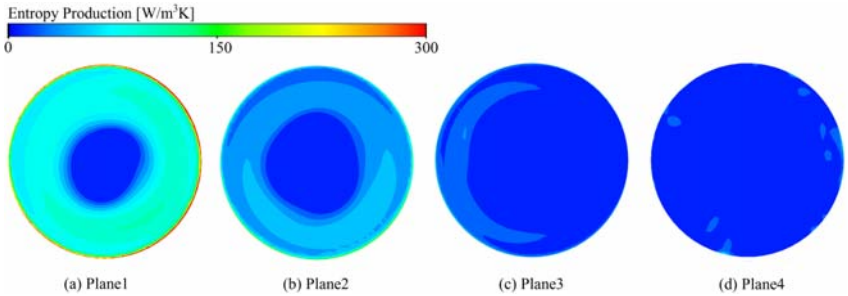

Fig. 19. Entropy production in inlet pipe when the bleed of casing treatment crosses the leading edge of the blades.

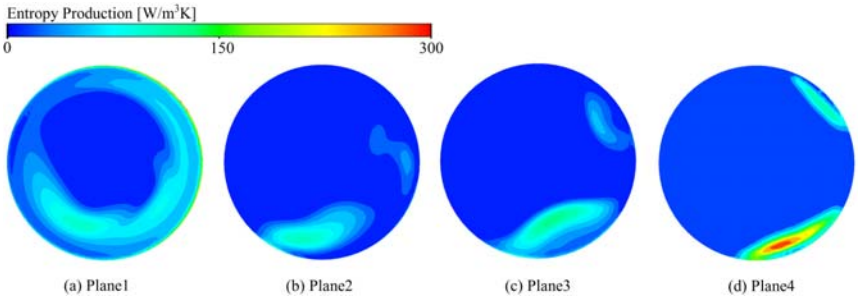

Fig. 20. Entropy production in inlet pipe when the bleed of casing treatment is under the leading edge of the blades.

further away from the leading edge, (Plane 4 is just to the left of the injector of the U-tube.) three high entropy areas appear, and they coincide with the three high energy stripes in Fig. 11, indicating that they are caused by the recirculated flow. When the bleed is located across the leading edge of the blades, Fig. 19, the losses in Planes 1-3 are almost as high as without the casing treatment, indicating a poor control of the back-flow. When the bleed is located under the leading edge of the blade, the losses in Plans 1 and 2 are reduced, and there are localized high entropy productions in Planes 3 and 4 particularly Plane 4, as shown in Fig. 20(c) and (d). Perhaps because of the bleed's closer vicinity to downstream volute and the higher recirculating flow velocity in this case, the asymmetric influence from the volute seems to feature strongly at the inlet pipe, helping to form these localized losses.

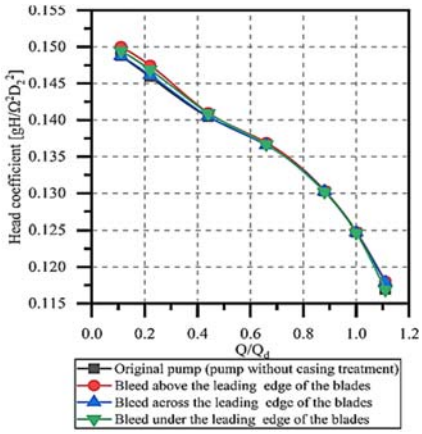

Fig. 21. Influence of the axial position of the bleed on head coefficient of the pump

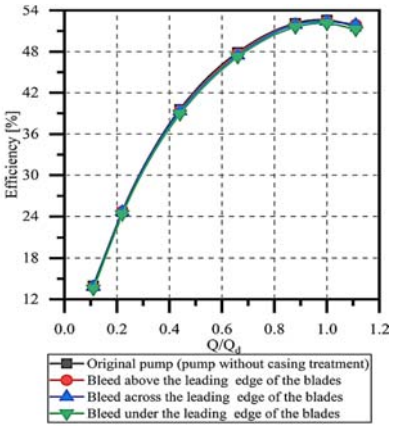

Fig. 22. Influence of the axial position of the bleed on efficiency of the pump

4.6 Influence of axial position on hydraulic performances of the studied pump

The head coefficient of the pump with and without casing treatment is illustrated in Fig. 21. It can be noticed that when bleed is located above and under the leading edge of the blades, the head coefficient of the pump improves when Q/Q_d is less than 0.44 which is also the flow condition when back-flow from impeller intensifies as shown in Fig. 5. This increment of the head coefficient implies an augmentation of impeller blade loading by the casing treatment through the suction of the back-flow and also the shroud end-wall boundary-layer. The least effective control of back-flow is when bleed crosses the leading edge of the blades, so there is little improvement in the head coefficient in this case. The influence of the axial position of the bleed on the efficiency of the pump is shown in Fig. 22. The casing treatment at different axial positions have little effect on the efficiency despite of the increase of the head coefficient; the losses within the U-tube and the mixing loss after the injector must have cancelled this benefit.

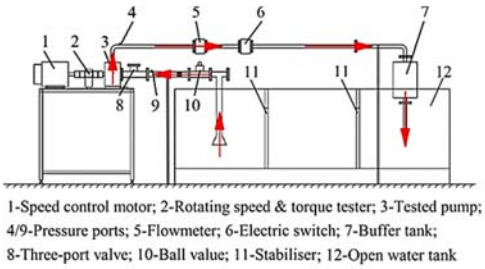

Fig. 23. Schematic of the experimental system.

5. EXPERIMENTAL VERIFICATION

5.1 Experimental system

The hydraulic experiment was carried out on an open type of centrifugal pump experimental system at Dalian Maritime University. Figure 23 shows the schematic diagram of the system and a photo of the system is shown in Fig. 24.

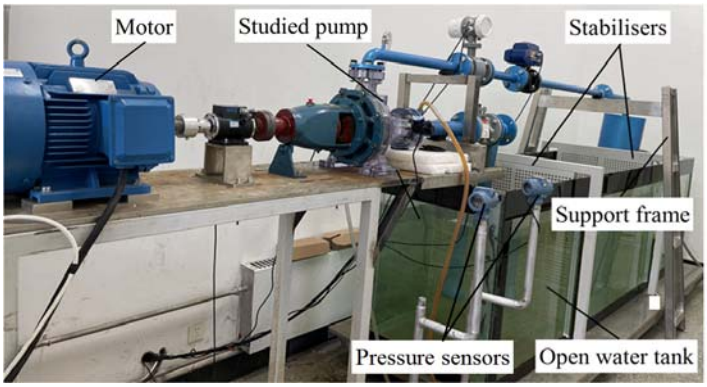

Fig. 24. Photo of the centrifugal pump experimental system.

The main components of the system consist of a data acquisition system (not shown), the speed controllable motor (1), the rotating speed & torque tester or torque meter with speed measurement (2),

the tested pump (3), the pressure ports (4 and 9), the flow meter (5), the electric switch or throttle (6) for controlling the flow of the pump, the open water tank (12) and the inlet & outlet pipes. To reduce or avoid vortices, pulsations and aeration in the inlet pipe caused by pump's discharge, a buffer tank (7) is installed at the line outlet. Two water stabilisers (11) are also installed for the same reason. To enable the installation of the U-tube casing treatment, the metal impeller was replaced with two 3D printed plexiglass ones, and the U-tube was built into one of them; the front part of the metal pump casing was also replaced with plexiglass one that incorporated with the casing treatment, as shown in Fig. 25.

5.2 Experimental results

Only the original pump (without casing treatment) and the same pump with the casing treatment where bleed is located above the leading edge of the blades (Fig. 3(a)), were tested. Experimental results from the test are shown in Fig. 26-27 where a comparison with numerical results of the pump is also made.

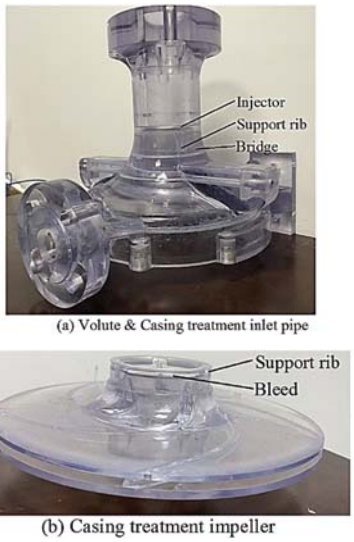

Fig. 25. Photos of 3D printed plexiglass pump with casing treatment.

It can be seen from the experimental results that the head coefficient of the pump is increased by the casing treatment and pump's efficiency is little affected by it. These findings are consistent with the numerical results given early on, and this gives some confidences to the conclusions drawn from the discussion of CFD results in previous sections.

Regarding the accuracy of the numerical results, the head coefficient and efficiency of the original pump obtained from the experiment are both lower than the simulation results. This may be expected as CFD simulations ignore the surface roughness of the pump casing and piping. (The surfaces of the 3D printed impeller were polished and are therefore smooth.) When the casing treatment is added, calculated pump efficiency is also slightly higher than measurement result, and the discrepancy can be tributed to the same reason. Measured head coefficient on the other hand is higher than numerical result when Q/Q_d is less than 0.6, and this needs a further investigation.

As can be seen in Fig. 16(a) and (b), there is a significant reduction in the low pressure zone in the inlet pipe after employing the casing treatment (bleed is located above the leading edge of the blades), implying that the casing treatment may improve the cavitation of the pump (2021). However, the CFD method used in this paper cannot capture any cavitation effects on the performance of pumps. In the case of this pump, some cavitation might exist at the inlet in the experiment at reduced mass flow conditions: the pump inlet is some distance above the water level in the tank and connects with the suction pipe through a 90° elbow, Fig. 22; and during the experiment the water entering the suction pipe was observed full of vortices because of the small size of the tank and strong disturbances caused by pump's discharge. Since cavitation will degrade a pump's performance, this may be another reason why in the original pump case, the simulation overpredicts the performance because it ignores the cavitation happening in the experiment; and this may also explain why when the casing treatment is employed, the simulation underestimates pump's performance

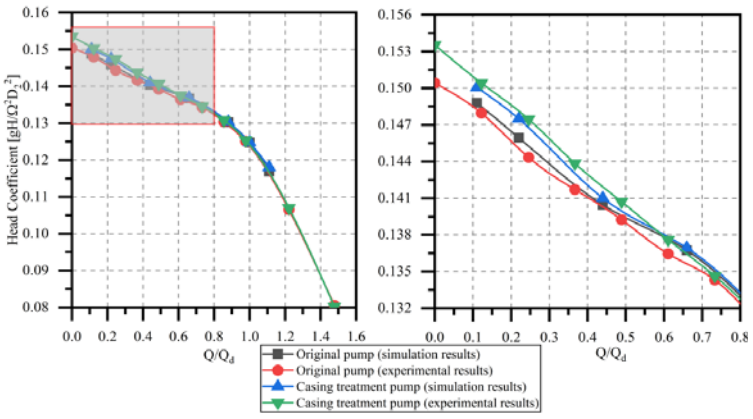

Fig. 26. Comparison of head coefficient of experimental and numerical results of the pump with and without casing treatment，enlarged view of shadowed area is shown on right.

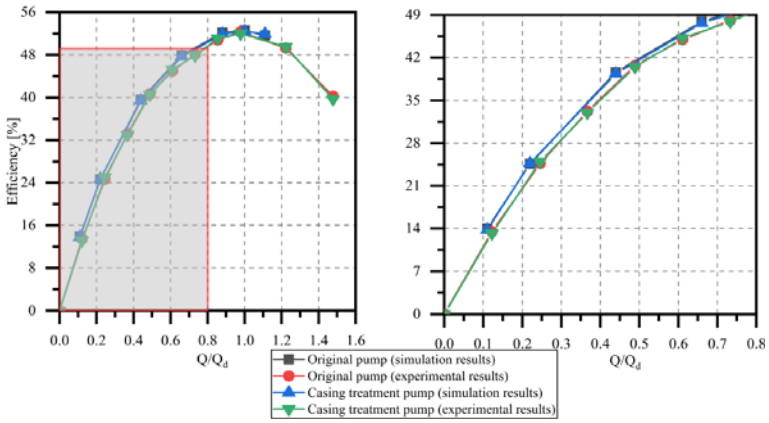

Fig. 27. Comparison of efficiency of experimental and simulation results of the pump with and without casing treatment，enlarged view of shadowed areas on right.

because the performance is greatly improved with the suppression of cavitation by the casing treatment.

6. CONCLUSIONS

In this paper, a self-circulating casing treatment is applied to a centrifugal pump, whereby the front cover of the impeller and the end-wall of the inlet pipe are both grooved to form a U-tube type fluid passage connecting the inlet of the impeller and pump inlet, and the influences of the axial position of the bleed of the U-tube on the performance of the centrifugal pump are investigated.

A steady CFD study was first carried out, which shows that the original pump undergoes back-flow at low mass flow conditions, and that a back-flow spreads over a progressively greater distance in the inlet pipe as the flow rate decreases and interferes with the main flow; that the U-tube sucks this back-flow near shroud end-wall and returns it to the pump inlet, due to the positive pressure gradient between its bleed and injector generated by the blade loading. It is found that when the bleed is located above or in front of the leading edge of the impeller, the blockage to the fluid in the U-tube is the smallest, so the suction is the strongest, and can effectively control the back-flow and increase the head coefficient of the studied pump; when the bleed is located under or behind the leading edge, the suction is the second best; and when the bleed crosses the leading edge, the blockage in U-tube is the most severe, the suction is the weakest, so too the control of the back-flow. It is also found that the fluid injected from the U-tube into the inlet pipe carried some positive circumferential velocity and high entropy, and the mixing of it with the incoming main flow generates losses. So, although the U-tube improves the flow in the impeller, the pump efficiency is little affected by the treatment.

An experimental study was performed with the original pump and the same pump with the casing treatment. A U-tube with its bleed located above the leading edge of the impeller was employed. The experimental results agreed well with the numerical results and verify the findings of this study. The results also show that the head coefficient of the pump is increased more than CFD prediction, and this is likely to do with the improvement of cavitation in the inlet region of the pump by the casing treatment in the experimental setup, which is ignored by the numerical simulation.

There are some limitations in this study. In this paper, we confirm the improvement of centrifugal pump back-flow and hydraulic performances by the casing treatment and reveal its control mechanism through numerical simulation and experimental methods. However, there are parts in need of refinement and further development. Firstly, the supporting ribs on centrifugal pump back-flow and performances improvement. The current selection of the supporting ribs is only considered to fix the spatial position of the U-tube and avoid resonance, so the supporting ribs are parallel to the pump shaft in the axial direction. This form of supporting ribs can not completely eliminate the pre-whirl carried by the back-flow. Therefore, the supporting ribs can be offset in the axial direction in the opposite direction of impeller rotating to further eliminate the pre-whirl, or even add reverse pre-whirl to the impeller inlet to further improve the hydraulic performances of the centrifugal pump. Secondly, the influence of casing treatment on cavitation. In this paper, it is found that the low pressure area in the inlet pipe and the leading edge of the impeller blade is significantly reduced after adding the casing treatment, as shown in Fig. 16, which means that the casing treatment can improve the anti-cavitation ability of the pump. Therefore, the influence of casing treatment on the cavitation of centrifugal pumps and the pressure pulsation generated by cavitation can be further explored by CFD and experimental methods.

ACKNOWLEDGMENTS

The authors disclose the receipt of the following financial support for the research, authorship, and/or publication of this article: This research is supported by the National Natural Science Foundation of China (Grant No. 51906027), the Doctoral Initiation Research Funds of Liaoning province (Grant No. 2019-BS-027)， the Fundamental Research Funds

for the Central Universities of China (No.3132019327) and the Fundamental Research Funds for the Central Universities (Grant No.3132020112).

REFERENCES

Chen, H. and V. M. Lei (2013). Casing treatment & inlet swirl of centrifugal compressors. *Journal of Turbomachinery* 135(04), 1-8.

Cheng, Q., W. M. Feng and L. C. Zhou (2016). Effect of front guide vane on the return vortex characteristics of axial flow pump saddle area operating conditions. *Journal of Agricultural Machinery* 47(4), 8-14.

Cooper, P., D. P. Sloteman and J. L. Dussourd (1984). Stabilization of the off-design behavior of centrifugal pumps and inducers. *Proceedings of the second European congress on fluid machinery for the oil, petrochemical and related industries.*

Feng, J. J., K. F. Yang, G. J. Zhu, X. Q. Luo and W. F. Li (2018). Axial grooving of inlet pipe wall surface to eliminate the characteristic curve hump of axial flow pump. *Journal of Agricultural Engineering* 34(13), 105-112.

Fraser, H. (1981). Flow recirculation in centrifugal pumps. US: *ASME meeting*.

Gonzalez, J., J. Fernandez, E. Blanco and C. Santolaria (2002). Numerical Simulation of the Dynamic Effects Due to Impeller-Volute Interaction in a Centrifugal Pump. *Journal of Fluids Engineering* 124(2).

Guo, L. (2019). *Study on the effect of leakage flow from the lobe top gap of semi-open centrifugal pumps on stall characteristics*. Shaanxi: Xi'an University of Technology.

Ito, Y., A. Tsunoda and Y. Kurishita (2015). Experimental Visualization of Cryogenic Back-flow Vortex Cavitation with Thermodynamic Effects. *Journal of Propulsion and Power* 32(01), 1-12.

Li, G., Y. Wang and P. Cao (2014). Numerical analysis of transient flow in centrifugal pump at off-design conditions. US: *6th International Symposium on Fluid Machinery and Fluid Engineering*.

Li, J. Q., W. W. Song, L. J. Wan and C. F. Shi (2019). Study on the mechanism of roughness on centrifugal pump inlet flow under multiple working conditions. *Thermal Power Engineering* 34(10), 63-70.

Li, Y., H. Chen, X. J. Li, M. H. Jiang and G. N. Wang (2020). The influence of casing treatment on the performance of a centrifugal pump. USA: *18th ISROMAC*.

Li, Y., H. Chen, X. J. Li, M. H. Jiang and G. N. Wang (2021). Influence of U-tube type casing treatment on pressure fluctuations of a centrifugal pump at low flow conditions. *Modern Physics Letters B*, 35(12).

Oshima, M. (1967). A study on suction performance of a centrifugal pump with an inducer [J]. *JSME* 10: 959–965.

Schiavelo, B. and M. Sen (1983). Performance prediction of centrifugal pump and compressors. US: *ASME 22nd Ann Fluids Engineering Conference.*

Si, Q., S. Yuan and J. Yuan (2013). Investigation on Flow-Induced Noise due to Back-flow in Low Specific Speed Centrifugal Pumps. *Advances in Mechanical Engineering* 109(5), 48-53.

Stepanoff, A. J. (1998). *Centrifugal and Axial Flow Pumps: Theory, Design, and Application*. Vienna: Springer.

Toyokura, T. and A. Kubota (1969). Studies on back-flow to the suction side of mixed-flow impeller blades. JSME;

Tsujimoto, Y. (1997). Observations of Oscillating Cavitation of an Inducer. *Journal of Fluids Engineering* 119(4), 775-781.

Tsujimoto, Y. (2007). Fluid Dynamics of Cavitation and Cavitating Turbo pumps. *Vienna: Springer.*

Tsujimoto, Y. (2013). Cavitation instabilities in hydraulic machines. *IOP Conference Series: Materials Science and Engineering* 52(1),169-190.

Tsujimoto, Y. and Y. Semenvo (2002). New types of cavitation instabilities in inducers. *Belgium: 4th International Symposium on Launcher Technology.*

Yamamoto, K. and Y. Sujimoto (2009). Backflow Vortex Cavitation and Its Effects on Cavitation Instabilities. *International Journal of Fluid Machinery & Systems* 2(01), 40-54.

Yuan, J. P., J. S. Hou, Y. X. Fu, J. W. Hu, H. Y. Zhang and C. D. Shen (2018). Study on the unsteady characteristics of back-flow vortex cavitation in a centrifugal pump. *Vibration and Shock* 37(16), 24-30.

Zhang, J. F., Y. Liang, J. P. Yuan and S. Q. Yuan (2012). *Numerical simulation of recirculation control at centrifugal pump inlet*. Jiangsu University 33, 402-407.